Biological Physics, 61–88

Poincaré Seminar 2009

Fluctuation Relations for Molecular Motors

David Lacoste and Kirone Mallick

Abstract. This review is focused on the application of specific fluctuation relations, such as the Gallavotti-Cohen relation, to ratchet models of a molecular motor. A special emphasis is placed on two-state models such as the flashing ratchet model. We derive the Gallavotti-Cohen fluctuation relation for these models and we discuss some of its implications.

1. Introduction

The macroscopic observables of a system at mechanical and thermal equilibrium do not vary with time and can be characterized by a finite number of state variables. Thermodynamics imposes *a priori* constraints on the average values of these state variables that are satisfied regardless of the specific nature of the system. Because of this property of time-invariance, equilibrium is often imagined as being associated with stillness and frozen dynamics. This, of course, is not true: a system, even at thermodynamic equilibrium, is constantly evolving from one micro-configuration to another. This endless motion at the microscopic level can be probed macroscopically by measuring the fluctuations of some physical observables, the most famous example being Brownian Motion. Equilibrium fluctuations are perfectly well explained by the classical laws of statistical mechanics.

Brownian motion, its nature, its origins, have been a puzzle to physicists during the XIXth century [1]. One paradoxical issue was the following: can one rectify this random fluctuating motion and use it to perform some work ? If such a rectifying device could be constructed then work would be extracted from a single heat reservoir, contradicting the second law of thermodynamics. The most famous example of a mechanical system that may play the role of such a Maxwell's demon is the ratchet and pawl system, presented by Feynman in Chapter 46 of the first volume of his Physics Lectures [2]. A related paradox was proposed in 1950 by Brillouin [3]: consider an electrical circuit composed of a diode and a resistor at temperature T. The current in the circuit has a zero average value, but because of thermal noise, it exhibits non-vanishing fluctuations (known as Johnson-Nyquist

noise). Can the diode be used to rectify the current, allowing us to use it to perform work? The solutions of these paradoxes are now well known: thermal fluctuations are a universal phenomenon and all systems at a given temperature are subject to it. The rectifying device, whatever it is, is also subject to Brownian motion and undergoes some unavoidable fluctuations. If the signal to be rectified is produced at temperature T and the rectifier is at the same temperature, then the thermal fluctuations of the rectifier render it totally ineffective and the second law is saved. If the rectifier is at a lower temperature then this apparatus can indeed generate work: but now there are two heat sources at different temperatures, in accordance with the second law.

In recent years, a renewed interest has arisen in ratchet models in the context of non-equilibrium statistical physics. Many ratchet models exist (for a review see [4]). In one kind of ratchet called brownian motors, an association of two particles, one asymmetric and another one symmetric, can rectify thermal fluctuations provided that the two particles are in contact with heat baths at different temperatures [5]. In another family of ratchet models, the need of two heat baths is removed by coupling the ratchet to some external 'agent' (e.g., a chemical reaction) that continuously drives the system out of equilibrium. In this case too, under certain conditions, work can be extracted [6, 7, 8]. Again, there is no contradiction with thermodynamics here: the system is far from equilibrium and the ratchet plays simply the role of a transducer between the energy put in by the agent (e.g., chemical energy) and the mechanical work extracted. The analysis of the energetics of such devices far from equilibrium requires concepts that go beyond the classical laws of thermodynamics and this remains a very challenging and important open issue [9, 10].

Biophysics provides numerous examples of systems far from equilibrium. For example, a significant part of the eukaryotic cellular traffic relies on 'motor' proteins that move along filaments similar in function to railway tracks or freeways (kinesins and dyneins move along tubulin filaments; myosins move along actin filaments) [11]. The filaments are periodic (of period $\sim$ 10nm) and have a fairly rigid structure; they are also polar: a given motor always moves in the same direction. These molecular motors appear in a variety of biological contexts: muscular contraction, cell division, cellular traffic, material transport along the axons of nerve cells... A biological cell forms a crowded environment in which molecular motors work together and with other proteins. In these conditions, collective effects arise due to interactions between motors [12]. In many cases, these interactions can be modeled as excluded volume interactions, and for this reason, the behavior of an ensemble of motors in a low dimension space can be described by dynamical models similar to the ones developed for traffic problems [13, 14]. In the following, we focus on single molecular motor properties, in order to clarify in this simpler situation, the dynamics and the energetics of this system far from equilibrium.

Recently, a general organizing principle for non-equilibrium systems has emerged which is known under the name of fluctuation relations [15, 16, 17, 18, 19, 20, 21]. These relations, hold for non-equilibrium steady states but arbitrarily far

from equilibrium [22, 23, 24, 25], they can be seen as macroscopic consequences of the invariance under time reversal of the dynamics at the microscopic scale [26]. It is interesting to apply these concepts to small systems which can either be mechanically driven as biopolymers [27] or chemically driven as enzymes [28].

Molecular motors are enzymes which operate stochastically at the level of a few molecules, and for this reason they typically undergo large thermal fluctuations. Generically, single molecular motors have been described theoretically either by continuous ratchet models (see, e.g., review by Jülicher et al. [29]) or by models based on master equations on a discrete space [30, 31]. It is possible to give a thermodynamic interpretation of the elementary chemical reactions, which occur in a discrete and stochastic way in a molecular motor [32]. Such a thermodynamic interpretation of chemical transitions has similarities with the thermodynamic interpretation of the Langevin equation at the single trajectory level [33]. At a macroscopic scale, constraints arise on the operation of these molecular motors, as a result of single reaction events occurring stochastically at the microscopic scale. These constraints take the form of a fluctuation relation [34, 32, 35, 36, 37, 38].

The aim of this review is to explain how recent theoretical results in non-equilibrium statistical mechanics, namely these fluctuation relations, provide a way to understand the non-equilibrium energetics of molecular motors. Note that the same framework apply to both biological molecular motors or artificially made nanomachines.

In the first part of this review, we present the two theoretical approaches of molecular motors mentioned above, namely the flashing ratchet model and the approach based on master equations on a discrete space. In the second part of the review, we derive the fluctuation relations for these specific models and discuss some consequences of these relations for molecular motors.

2. Stochastic models of molecular motors

Molecular motors are enzymes capable of converting chemical energy derived from the hydrolysis of adenosine triphosphate (ATP) into mechanical work. There is a large diversity of molecular motors, and correspondingly a large number of processes accomplished by these motors within a cell. There are linear motors such as kinesins, dyneins, myosins or the RNA polymerases, and rotating motors such as the F_1-ATPase motor or the bacterial flagellar motor. These motors drive not only intracellular movements, they are also key players in the motility of the cell itself. Although, traditionally, these machines were subjects of investigation in biology and biochemistry, increasing use of the concepts and techniques of physics in recent years have contributed to a quantitative understanding of the fundamental principles of operation of these motors. The possibility of exploiting these principles for the design of artificial nanomachines has opened up a new field in nanotechnology.

2.1. The basic principle

On the theoretical side, molecular motors have been described by ratchet devices, which are systems able to extract useful work out of unbiased random fluctuations [39]. A generic model of such a ratchet device is shown in Figure 1 where the motor is represented by a small particle that moves in a one-dimensional space. At the initial time $t = 0$, the motor is trapped in one of the wells of a periodic asymmetric potential of period a. Between time 0 and t_f, the asymmetric potential is erased and the particle diffuses freely and isotropically at temperature T. At the switching time t_f, the asymmetric potential is re-impressed, the motor slides down to the nearest potential valley and, because of damping, is trapped in one of the wells. The motor has maximal chance to end up in the same well where it was at time $t = 0$. However, it has a small probability to be trapped in the well located to the right and, because of the asymmetry of the potential, an even smaller probability to end up in the left well. Indeed, in order to be trapped in the right well after time t_f, the particle must have diffused between $t = 0$ and $t = t_f$ over a distance larger than A towards the right. However, to end up in the left well it has to diffuse (towards the left) a distance larger than B, which is much less probable because $B > A$. In other words, because the potential is asymmetric, the motor has more chances to slide down towards the right: this leads on average to a net total current. The particle has used thermal noise to overcome the potential barrier and thanks to the asymmetry of the potential it has moved in a well-defined direction.

In order to move, the motor consumes r ATP fuel molecules per unit time, which are hydrolyzed to ADP + P (see Figure 2):

$$ATP \rightleftharpoons ADP + P\,.$$

It is the chemical energy released by ATP-hydrolysis that allows the motor to detach itself from the filament it was bound to. This detachment process corresponds in the basic mechanism to erasing the potential, whereas re-attachment of the motor at the switching time t_f corresponds to re-impressing the potential. Hence the motor undergoes chemistry-driven changes between strongly and weakly bound states (attachments and detachments). It is the coupling between chemistry and the interaction with the filament that allows the motor to overcome energy barriers. Besides, because of the polarity of the filament, the interaction potential is asymmetric, allowing directed motion to set in.

In general, the motor is subject to an external force $f_{\rm ext}$ which tilts the potential. Besides, when ATP is in excess, the chemical potential difference of the reaction of ATP hydrolysis, $\Delta\widetilde{\mu} = \mu_{\rm ATP} - \mu_{\rm ADP} - \mu_{\rm P}$ becomes *positive*. More precisely, we denote $\Delta\widetilde{\mu} \equiv k_B T \Delta\mu$, where $\Delta\mu$ is the normalized chemical potential and

$$\Delta\tilde{\mu} = k_B T \ln\left(\frac{[ATP]\,[ADP]_{\rm eq}\,[P]_{\rm eq}}{[ATP]_{\rm eq}\,[ADP]\,[P]}\right), \tag{1}$$

where [..] denotes concentration under experimental conditions and $[..]_{\rm eq}$ denotes equilibrium concentrations.

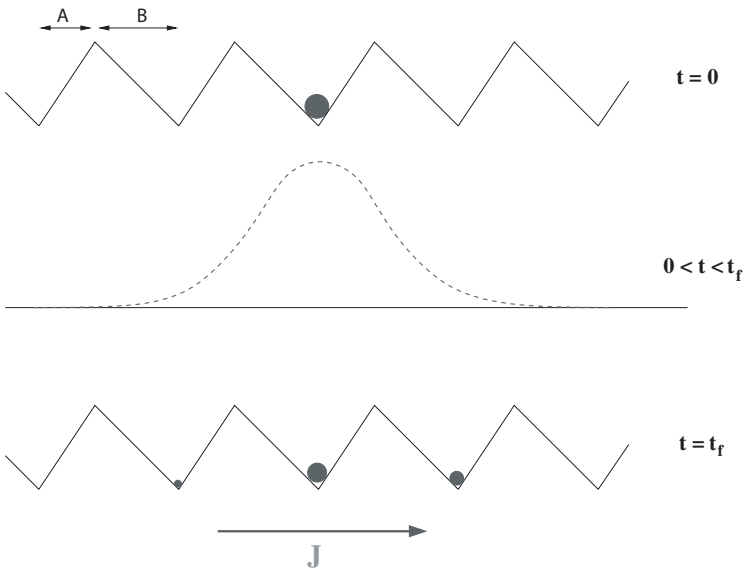

FIGURE 1. The principle of a Brownian ratchet: by inscribing and erasing periodically an asymmetric potential, a directed motion of the particle is induced. In this example, the potential is a saw-tooth function of period $a = A + B$. Since $B > A$, the potential is asymmetric. The relative sizes of the probabilities of ending in one of the wells are represented by the sizes of the disks in the lowest picture. The right and left probabilities being different, this leads on average to a net total current J.

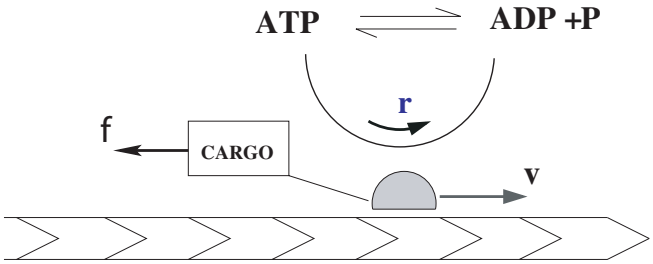

FIGURE 2. Schematic representation of a molecular motor: by hydrolyzing ATP, the motor proceeds along the polar filament and carries a 'cargo' molecule, which typically exerts a force f on the motor.

A basic problem is then to determine the velocity of the motor $v(f_{\text{ext}}, \Delta\mu)$ (mechanical current) and the ATP consumption rate $r(f_{\text{ext}}, \Delta\mu)$ (chemical current) as functions of the external mechanical and chemical loads.

To summarize, molecular motors move by using the ratchet effect, providing an example of a *rectification process* of Brownian motion. The two basic requirements for obtaining directed motion are:

(i) an external energy source, provided by the chemical reaction of ATP hydrolysis. During this process ATP is consumed and ADP is produced. This reaction therefore breaks time-reversal invariance (more technically, it breaks the detailed balance condition which holds at equilibrium, and introduces a bias in the dynamics of the motor).
(ii) The polarity of the filament which breaks spatial left-right symmetry and allows the motor to move in a well-defined direction.

2.2. The flashing ratchet model

In the simplified discussion above, we did not specify the characteristics of the switching time t_f. Different models are possible: one can consider a deterministically forced ratchet in which the binding potential of the motor switches periodically (and even smoothly) from strong-binding to weak-binding. Another possibility that we shall discuss here in detail is the flashing ratchet model [29, 4] in which the switching of potentials is sudden and occurs at random times generated by a Poisson Process. Then, we shall show how to construct a discrete version of the flashing ratchet model [30, 31].

In the flashing ratchet model [29, 40, 41], the state of the motor is described by a continuous position variable x and by discrete internal states $i = 1, 2$ corresponding to different chemical states of the motor. For instance, one could associate one state with a configuration where one motor head is bound to the filament (the high-energy state) and the other state to a configuration where both heads are bound (the low-energy state). The motor evolves in two time-independent periodic potentials $U_i(x)$, with $i = 1, 2$. Note that in the basic mechanism discussed in the previous section, $U_1(x)$ is a saw-tooth potential and $U_2(x)$ is taken to be zero. But one can consider the general case where both U_1 and U_2 are non-zero asymmetric potentials of arbitrary shape with a common period a. In Figure 3, we represent the often studied situation in which U_1 and U_2 are identical saw-tooth potentials but slightly shifted with respect to each other along the x axis.

The dynamics of the motor can be represented by a Langevin equation

$$\dot{x} = -\gamma F - \gamma \sum_{i=1,2} U_i(x)\delta_{\zeta(t),i} + \sqrt{D_0}\,\xi(t) \tag{2}$$

where $\xi(t)$ is a normalized white-noise and $\zeta(t)$ a dichotomous noise that can exist in two states 1 and 2. The switching-rates of $\zeta(t)$ are position dependent and are given by $\omega_1(x)$ (transition from 1 to 2) and $\omega_2(x)$ (transition from 2 to 1). The friction coefficient γ satisfies the Einstein relation $D_0 = k_B T/\gamma$ and F represents an external force acting on the motor. The function $\delta_{\zeta(t),i}$ is a Kronecker delta.

The probability density for the motor to be at position x at time t and in state i is denoted by $P_i(x,t)$, which obeys the equations

$$\frac{\partial P_1}{\partial t} + \frac{\partial J_1}{\partial x} = -\omega_1(x)P_1 + \omega_2(x)P_2, \tag{3}$$

$$\frac{\partial P_2}{\partial t} + \frac{\partial J_2}{\partial x} = \quad \omega_1(x)P_1 - \omega_2(x)P_2\,, \tag{4}$$

where $\omega_1(x)$ and $\omega_2(x)$ are space dependent transition rates, and the local currents J_i are defined by:

$$J_i = -D_0\left(\frac{\partial P_i}{\partial x} + \frac{1}{k_BT}\left(\frac{\partial U_i}{\partial x} - F\right)P_i\right), \tag{5}$$

with D_0 the diffusion coefficient of the motor and F a non-conservative force acting on the motor.

The transition rates can be modeled using standard kinetics for chemical reactions applied to each chemical pathway between the two states of the motor [40]:

$$\begin{aligned}\omega_1(x) &= [\omega(x) + \psi(x)e^{\Delta\mu}]e^{(U_1(x)-fx)/k_BT},\\ \omega_2(x) &= [\omega(x) + \psi(x)]e^{(U_2(x)-fx)/k_BT},\end{aligned} \tag{6}$$

where $f = Fa/k_BT$ is the normalized force acting on the motor. It is assumed that the rates can be decomposed into a contribution proportional to $\omega(x)$, which is associated with thermal transitions, and a contribution proportional to $\psi(x)$ corresponding to transitions induced by ATP hydrolysis. Note that the functions $\omega(x)$ and $\psi(x)$ have to be periodic functions but they are otherwise unspecified. The form of the rates in the absence of hydrolysis (*i.e.* when $\psi(x) = 0$) is chosen to satisfy the detailed balance condition

$$\frac{\omega_2(x)}{\omega_1(x)} = \exp\left(\frac{U_2(x) - U_1(x)}{k_BT}\right). \tag{7}$$

The form of the rates associated with the transitions induced by ATP hydrolysis (*i.e.* when $\omega(x) = 0$) is chosen to satisfy a generalized detailed balance condition, which is generalized in the sense that it accounts for the exchange of chemical energy [35, 28]. In this case, this leads to the condition

$$\frac{\omega_2(x)}{\omega_1(x)} = \exp\left(\frac{U_2(x) - U_1(x)}{k_BT} - \Delta\mu\right). \tag{8}$$

Note that the way the force enters the rates is unambiguous in continuous models as compared to discrete models, in which the force dependent rates must contain unknown load distribution factors [37, 30]. One could easily extend the model to introduce more chemical pathways [40] or more internal states; such extensions are possible but they have not been considered here since they are not essential for the present argument.

When $F = 0$ and $\Delta\mu = 0$, the system is in equilibrium since the detailed balance condition (7) holds. In this case, the steady state probabilities P_i obey

Boltzmann distribution, the currents J_i vanish and there is no average displacement of the motor. When F and $\Delta\mu$ are not simultaneously zero, the detailed balance condition (7) is broken, the system is out of equilibrium and currents are present.

2.3. A discrete ratchet model

From the continuous model, a simplified effective discrete model can be constructed as shown schematically in Figure 3 following the procedure outlined in [42]. We as-

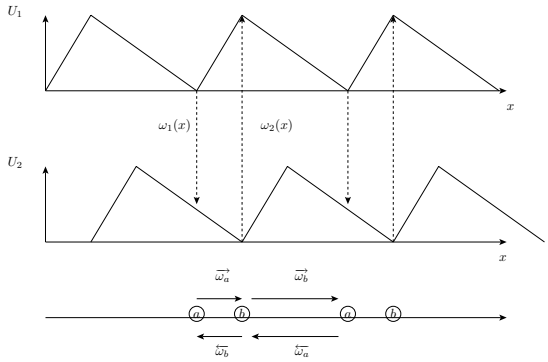

FIGURE 3. The top two curves represent the two time independent periodic potentials $U_1(x)$ and $U_2(x)$ of the flashing ratchet model. At any position x, vertical transitions are possible between the two internal states with rates $\omega_1(x)$ and $\omega_2(x)$. Below is represented the corresponding discrete model, which is obtained by considering effective transitions between the minimum of $U_1(x)$ (state a) to the minimum of the other potential (state b), with rates as shown in the lower part of the figure.

sume that the motor has a vanishingly small residence time in all states which are not minima of the potentials $U_1(x)$ or $U_2(x)$, i.e. the time taken to slide down towards a well is negligible. Switching between the potentials, represented as dashed lines in the figure, occurs at finite rates $\omega_1(x)$ and $\omega_2(x)$, but only between states that are at the same location x. Since downward sliding occurs instantly, the observable transitions are effectively from one minimum of one potential (state a) to the other minimum of the other potential (state b). In this way, a discrete hopping model on a 1D lattice is constructed in which transitions are allowed between even and odd sites called a and b. The dynamics of the motor on the linear discrete lattice is as follows: the motor hops from one site to neighboring sites, either consuming or producing ATP (see Figure 4). The position of the motor is denoted by $x = nd$, where $2d \approx 8\,\text{nm}$ is the step size of a kinesin. The even sites (denoted by a) are the low-energy state of the motor, whereas the odd sites (denoted by b) are its high-energy state; their energy difference is $\Delta E \equiv k_B T\epsilon$, where k_B is the Boltzmann constant and T is the temperature. Because of the periodicity of the

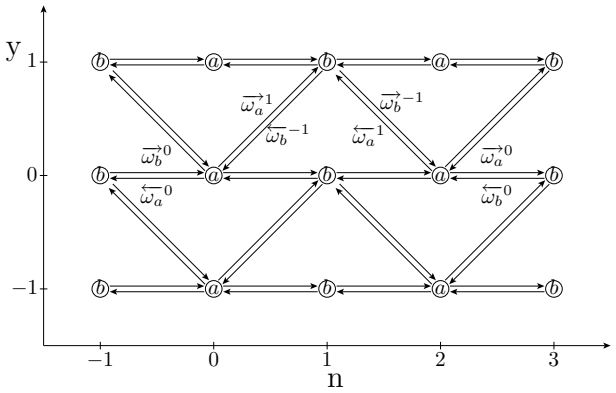

FIGURE 4. A schematic of the evolution of the motor in a plane (n, y), where n represents the position of the motor on the filament and y is the number of ATP molecules consumed. The even and odd sublattices are denoted by a and b, respectively. Note that the lattices of a and b sites extend infinitely in both directions along the n and y axis. The possible transitions are represented with arrows on a particular section of the lattice.

filament, all the even (a) sites and all the odd (b) sites are equivalent. The dynamics of the motor is governed by a master equation for the probability, $P_n(y,t)$, that the motor has consumed y units of ATP and is at site n at time t:

$$\begin{aligned}\partial_t P_n(y,t) = & -(\overleftarrow{\omega}_n + \overrightarrow{\omega}_n)\, P_n(y,t) \\ & + \sum_{l=-1,0,1} \left[\overleftarrow{\omega}_{n+1}^{\,l}\, P_{n+1}(y-l,t) + \overrightarrow{\omega}_{n-1}^{\,l}\, P_{n-1}(y-l,t) \right], \end{aligned} \tag{9}$$

where $\overleftarrow{\omega}_n \equiv \sum_l \overleftarrow{\omega}_n^{\,l}$ and $\overrightarrow{\omega}_n \equiv \sum_l \overrightarrow{\omega}_n^{\,l}$. Denoted by $\overleftarrow{\omega}_n^{\,l}$ and $\overrightarrow{\omega}_n^{\,l}$ are the transition rates for the motor to jump from site n to $n-1$ or to $n+1$, respectively, with $l\,(=-1,0,1)$ ATP molecules consumed.

As we show below, this discrete stochastic model contains the essential features of the original ratchet model while being more amenable to precise mathematical analysis [43, 44, 45, 31]. In this sense, the discrete model may be regarded as a *minimal* ratchet model.

2.4. Application of the model to experiments

2.4.1. Modes of operation and efficiency: From the master equation Eq. 9, one can obtain the average velocity of the motor $\bar{v}$ and its average ATP consumption rate, $\bar{r}$. One finds explicitly that

$$\bar{v} = 2\frac{\overrightarrow{\omega}_a \overrightarrow{\omega}_b - \overleftarrow{\omega}_a \overleftarrow{\omega}_b}{\overrightarrow{\omega}_a + \overrightarrow{\omega}_b + \overleftarrow{\omega}_a + \overleftarrow{\omega}_b}\,, \tag{10}$$

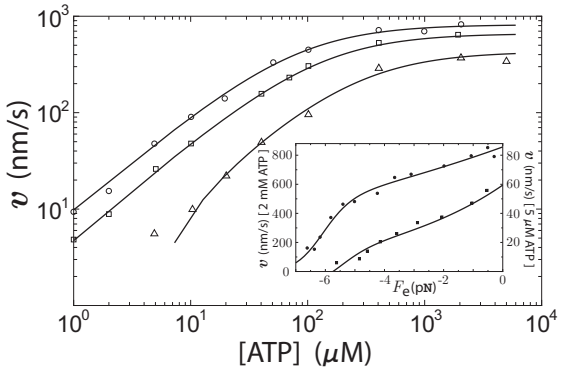

FIGURE 5. Kinesin velocity vs. ATP concentration under an external force [36]. The solid curves are the fits of our model to data from Ref. [46]. From top to down, the plots are for $F_e = -1.05, -3.59$, and $-5.63\,\mathrm{pN}$, respectively. Inset: Kinesin velocity vs. force under a fixed ATP concentration. The solid curves are fits to the data of Ref. [46]. From top to down, the plots are for $[\mathrm{ATP}] = 2\,\mathrm{mM}$ and $5\,\mu\mathrm{M}$.

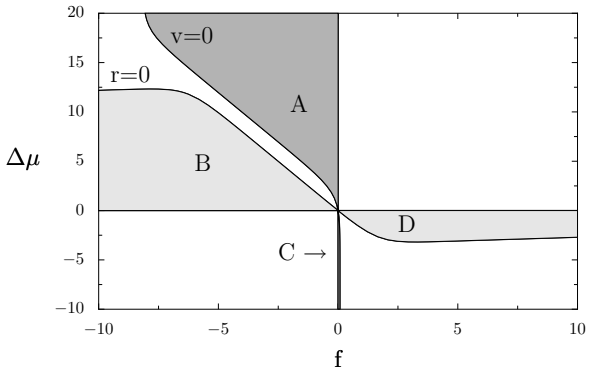

FIGURE 6. The four modes of operation of a molecular motor (such as kinesin) are delimited by $\bar{v} = 0$ and $r = 0$. The lines are generated with parameters that we have extracted by fitting the data for kinesin in Ref. [46] to our model, and this fit is shown in Figure 5.

$$r = \frac{\left(\overleftarrow{\omega}_a^{\,1} + \overrightarrow{\omega}_a^{\,1}\right)\left(\overrightarrow{\omega}_b + \overleftarrow{\omega}_b\right) - \left(\overleftarrow{\omega}_b^{\,-1} + \overrightarrow{\omega}_b^{\,-1}\right)\left(\overrightarrow{\omega}_a + \overleftarrow{\omega}_a\right)}{\overrightarrow{\omega}_a + \overrightarrow{\omega}_b + \overleftarrow{\omega}_a + \overleftarrow{\omega}_b}\,. \tag{11}$$

By modelling the dependence of the rates on the force and on the chemical potential in a way similar to what was done in Eq. (6) for the flashing ratchet model, one obtains a theoretical prediction for the dependence of the velocity and

average ATP consumption rate on the force or the ATP concentration, that can be compared to experiments. Despite its simplicity, this discrete model can account quantitatively for such measurements as shown in Figure 5 in the case of a kinesin.

From the two currents $\bar{v}$ and r, a diagram of operation of the motor (see Figure 6) can be constructed, which summarizes the possible thermodynamic modes of operation of the motor [36]. This diagram is similar to that given in Ref. [29], except that the present diagram extends to the regime far from equilibrium rather than being limited to the linear response regime. Whenever $f\bar{v} < 0$, work is performed by the motor, whenever $r\Delta\mu < 0$, chemical energy is generated. The motor can work in eight different regimes. Four of them are passive and correspond to the white regions in Figure 6, in which there is no energy output from the system, since $f\bar{v} > 0$ and $r\Delta\mu > 0$. [1] The four remaining regimes are more interesting since $f\bar{v}$ and $r\Delta\mu$ are not of the same sign, which means that some form of transduction occurs between the mechanical and chemical forms of energy. More precisely:

- In region A of the diagram, where $r\Delta\mu > 0$ and $f\bar{v} < 0$, the motor uses the chemical energy of ATP to perform mechanical work. This can be understood by considering a point on the y-axis of Figure 6 with $\Delta\mu > 0$. There we expect that the motor drifts to the right with $\bar{v} > 0$. Now in the presence of a small load $f < 0$ on the motor, we expect that the motor is still going in the same direction although the drift is uphill and thus work is performed by the motor at a rate $\dot{W} = -f\bar{v} > 0$. This holds as long as f is smaller than the stalling force, which defines the other boundary of region A.
- Similarly, in region B, where $r\Delta\mu < 0$ and $f\bar{v} > 0$, the motor produces ATP already in excess from mechanical work.
- In region C, where $r\Delta\mu > 0$ and $f\bar{v} < 0$, the motor uses ADP in excess to perform mechanical work.
- In region D, where $r\Delta\mu < 0$ and $f\bar{v} > 0$, the motor produces ADP already in excess from mechanical work.

It is interesting to note that the large asymmetry between regions A and C in Figure 6 reflects the fact that kinesin is a unidirectional motor. The diagram also illustrates the fact that under usual conditions with $\Delta\mu \simeq 10 - 25$, a kinesin uses the chemical energy of ATP hydrolysis to produce mechanical work (region A of the figure), rather than operating in the other way to synthesize ATP (region B of the figure).

It is also possible to analyze the mechanical efficiency of this motor, defined as the ratio between the mechanical work delivered by the motor divided by the chemical energy supplied [37]. Other definitions of efficiency have been considered in the literature (such as the efficiency at maximum power [47] or the Stokes efficiency) but the advantage of this definition is that it holds arbitrarily far from

[1] The case where $f\bar{v} < 0$ and $r\Delta\mu < 0$ is forbidden by the second law of thermodynamics, because it would lead to a negative entropy production. For this reason, there is no point in Figure 6 which corresponds to this case.

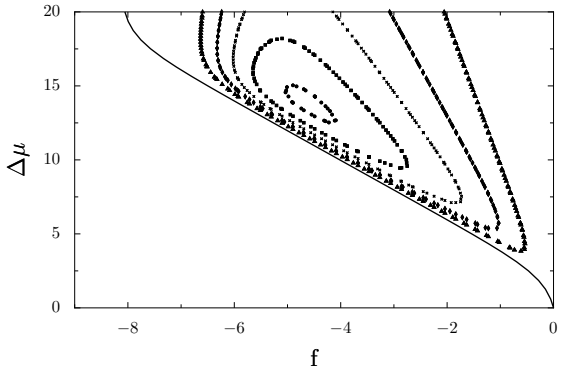

FIGURE 7. Curves of equal efficiency η within region A (which is delimited by the solid line and by the y axis). The parameters are those used in Figure 6 and obtained from the fit of Figure 5. From the outside to the inside the curves correspond to $\eta = 0.2$, $\eta = 0.3$, $\eta = 0.4$, $\eta = 0.5$ and $\eta = 0.58$. The absolute maximum efficiency for these parameters is about 59% and is located at $\Delta\mu \simeq 14$ and $f \simeq -4.9$.

equilibrium and it corresponds near to equilibrium to the definition used traditionally with heat engines. The kinesin operates most efficiently in a range of values of $\Delta\tilde{\mu}$ which corresponds well to the typical free energy delivered by the reaction of ATP hydrolysis (physiological conditions correspond to $\Delta\mu \simeq 10 - 25$). The maximum of efficiency is obtained around a single isolated point in the coordinates $(f, \Delta\mu)$ (rather than on a line as in the near equilibrium regime for instance) as shown in Figure 7. This suggests that kinesin is in fact optimized to operate under a load corresponding to a normalized force of about -4.9 in the conditions of Figure 7. The maximum of efficiency is around 40–60%, much higher than the typical efficiency in the near equilibrium regime (of the order of 0.03%). The value of the maximum efficiency of 40–60% agrees well with recent measurements for kinesin.

2.4.2. Violation of Onsager and Einstein relations: Away from equilibrium, we expect that Onsager and Einstein relations are no longer valid. To quantify their violations, we have introduced in Ref. [36] $\Delta\lambda \equiv \lambda_{12} - \lambda_{21}$ to quantify the violation of Onsager relations and four "temperature"-like quantities, $T_{ij} \equiv D_{ij}/\lambda_{ij}$ to quantify the violation of Einstein relations. All these quantities are defined using linear response theory in the vicinity of a non-equilibrium steady state rather than near an equilibrium state. Of course, these effective temperatures are not thermodynamic temperatures: they are merely one of many possible ways to quantify deviations of Einstein relations. These T_{ij} and $\Delta\lambda$ are shown in Figure 8 as functions of $\Delta\mu$ for the particular case of $f \ll 1$ within region A. We observe that all the T_{ij} start off at $T_{ij} = 1$ near equilibrium where $\Delta\lambda = 0$ as expected from

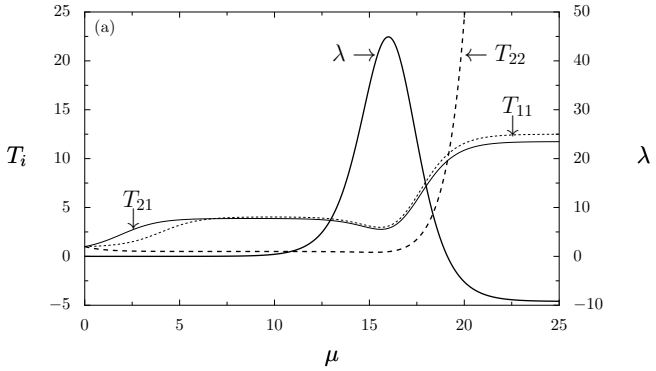

FIGURE 8. Effective temperatures T_{11} (dot-dashed), T_{21} (dotted), T_{22} (dashed), and $\Delta\lambda$ (solid) vs. $\Delta\mu$ in region A of Figure 6 for a small f. Note that T_{ij} characterizes the fluctuation-response ratios (see text), while $\Delta\lambda$ quantifies the breaking of Onsager symmetry.

Onsager relations, whereas for large $\Delta\mu$, T_{22} diverges exponentially while T_{21}, T_{11} and $\Delta\lambda$ approach constant values [36].

2.4.3. Beyond two states model of molecular motors. The discrete two-state model presented above describes many features of experiments on a single kinesin such as the average velocity versus force or versus ATP concentration, or the average ATP consumption rate. It does not describe however equally well the fluctuations of these quantities. As shown in [30], at least four internal states are necessary to describe the fluctuations of position of the motor, which are quantified by the so-called randomness parameter introduced and measured in Ref. [48]. For this reason, a more refined model of kinesin should contain more than two internal states to account for the way the motor walks on the filament, which is by a succession of binding and unbinding events of the two heads in a hand-over-hand fashion. To include that aspect, a model with nine states – which can be reduced to seven states for most cases – was proposed in Refs. [35, 49, 50], where the seven states describe the most significant chemical states of the two headed kinesin. The possible transitions between these states can be represented by a network, which describes the mechano-chemical coupling in this motor. In this network representation, several cycles can be identified just like in the discrete model presented above. The model successfully accounts for many experimental results known for kinesins [51]. Using this framework, a diagram summarizing the thermodynamic modes of operation of the motor has been constructed in Ref. [52]. This diagram has similarities with our Figure 6, but some differences are present due to the different role played by the mechanical and chemical cycles in the different models.

Many other works have used discrete or continuous stochastic models to analyze molecular motors: for instance a discrete model with seven states has been

developed for myosin V [53]. A discrete model with only three states has been used to describe the fluctuations of position of nucleosomes along DNA in Ref. [55]. In Ref. [54], the rotating motor F_1-ATPase is described by a stochastic process for the angle of rotation of the motor, which is treated as a continuous variable and for the chemical states, which are treated as discrete states. More recently, the authors of this reference have developed a discrete version corresponding to their continuous model, which is a two-state model very similar to the one discussed in this review [56].

3. Fluctuation relations in models of molecular motors

Fluctuation relations quantify the exchanges of energy between a system and its environment when the system is in a non-equilibrium state [17, 21]. These relations hold arbitrarily far from equilibrium in a regime where the usual thermodynamic laws – which hold only near equilibrium – do not apply. Since their discovery about a decade ago [15, 16, 17, 18, 19], there has been a growing interest in understanding their importance and implications. One reason for the popularity of this topic has to do with the fact that these relations provide a fresh look at old fundamental questions, such as the origin of irreversibility or the second law of thermodynamics.

For small systems (for which the fluctuations are large, in the sense that their magnitude can be of the same order as the average value), the fluctuation relations impose new constraints which go beyond the usual description of statistical fluctuations. Many fluctuation relations have been verified experimentally using biopolymers, in particular the Jarzynski's relation [57], the Crooks relation [58] and the Hatano-Sasa relation [59]. Complementary experimental verifications have been carried out with colloidal particles in optical traps [60, 61]. Recently, a modified Fluctuation-Dissipation relation, related to the Hatano-Sasa relation has been verified for a colloidal particle in a nonequilibrium steady state [62]. All these experiments represent remarkable achievements, which confirm the validity of the general framework of fluctuation relations in various experimental conditions. However, it may be worth pointing out that in all these examples, the experiments have been designed in order to verify the fluctuation relations. On the contrary, the case of molecular motors is particularly interesting since this is a system which was not designed for that objective. Molecular motors operate in a regime far from equilibrium, with fluctuation relations in some sense built-in in their natural mode of operation. For this reason, it is more appropriate to think about fluctuation relations as thermodynamic constraints on the operation of the motors, which presumably theoretical models of molecular motors should obey [34, 32]. That of course would assume that the fluctuation relations are obeyed exactly in experiments. To our knowledge, quantitative experimental tests of fluctuation relations have not been carried out on molecular motors yet, although there is some indication that, for instance, the data of [51] on single molecule experiments with kinesin is in agreement with the fluctuation relations.

The dynamics of a molecular motor breaks the detailed balance condition, and leads to a non-equilibrium steady state characterized by the presence of non-zero currents, which are independent of time. For each current, one can associate a cycle, also called an irreversible loop. The construction of these cycles and the way they can be associated with currents is explained by a general theory for systems governed by a master equation [63, 65, 64]. One central result of this theory is the relation

$$\frac{\Pi^+(\mathcal{L})}{\Pi^-(\mathcal{L})} = \frac{J^+}{J^-} = e^{A/k_BT}, \tag{12}$$

where $\Pi^+(\mathcal{L})$ denotes the product of reaction rates associated with the different transitions within the cycle $\mathcal{L}$ in the clockwise direction, whereas $\Pi^-(\mathcal{L})$ denotes the same product in the counter-clockwise direction. We have denoted by J^+ the number of cycles undergone by the motor per unit time in the clockwise direction, and J^- the number of cycles undergone per unit time in the counter-clockwise direction, so that overall the cycle flux is $J = J^+ - J^-$. The quantity A is called affinity or thermodynamic force. This affinity can be defined as the derivative of an effective potential, experienced by a biased random walker that would exhibit the same dynamics [37]. When the detailed balance condition is satisfied, $\Pi^+(\mathcal{L}) = \Pi^-(\mathcal{L})$, the effective potential is flat and $A = J = 0$.

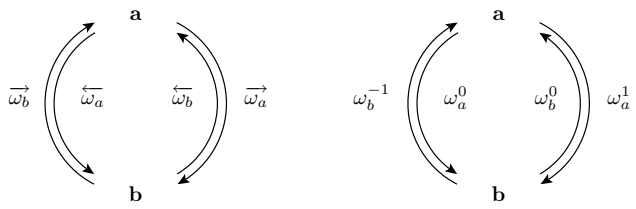

FIGURE 9. Cycles associated with the evolution of the motor in the discrete two-state model. Left: the cycle for the position variable n; the length n run by the motor corresponds to half the number of turns run around the cycle (the factor $1/2$ has to do with the period of the motor which is twice the unit length of the lattice on which the motor evolves). Right: the cycle for the chemical variable y.

In the simple case where the model contains a single cycle with only two states as in Figure 9, the relation (12) leads to the affinity $A/k_BT = -2\Psi$ where Ψ is defined by

$$\Psi = \frac{1}{2} \ln \left(\frac{\overleftarrow{\omega}_a \overleftarrow{\omega}_b}{\overrightarrow{\omega}_a \overrightarrow{\omega}_b} \right), \tag{13}$$

and the corresponding current J is the average motor velocity (see Eq. 10):

$$\bar{v} = 2 \frac{\overrightarrow{\omega}_a \overrightarrow{\omega}_b - \overleftarrow{\omega}_a \overleftarrow{\omega}_b}{\overrightarrow{\omega}_a + \overrightarrow{\omega}_b + \overleftarrow{\omega}_a + \overleftarrow{\omega}_b}. \tag{14}$$

In order to describe more precisely the dynamics of this system, let us consider $P_i(n,t)$, the probability that the motor at time t is on the site i $(= a, b)$ and at the position n (with $x = nd$ where d is distance between sites a and b). This probability can be obtained for instance by integrating over the variable y in the quantity $P_n(y,t)$, which satisfies the more general master equation of Eq. (9). Because of the periodicity of this problem, it is convenient to introduce generating functions $F_i(\lambda,t) \equiv \sum_n e^{-\lambda n} P_i(n,t)$, which evolve according to : $\partial_t F_i = \mathcal{M}_{ij}\, F_j$, where $\mathcal{M}[\lambda]$ is the following 2×2 matrix constructed from the master equation satisfied by $P_i(n,t)$:

$$\mathcal{M}[\lambda] = \begin{bmatrix} -\overrightarrow{\omega_a} - \overleftarrow{\omega_a} & e^{\lambda}\,\overleftarrow{\omega_b} + e^{-\lambda}\,\overrightarrow{\omega_b} \\ e^{\lambda}\,\overleftarrow{\omega_a} + e^{-\lambda}\,\overrightarrow{\omega_a} & -\overleftarrow{\omega_b} - \overrightarrow{\omega_b} \end{bmatrix}.$$

In the long time limit, the steady state properties of the motor can be obtained from the largest eigenvalue $\vartheta[\lambda]$ of this matrix. Indeed when $t \to \infty$,

$$\left\langle\, e^{-\lambda n} \,\right\rangle = \sum_i F_i(\lambda,t) \sim \exp\left(\vartheta\, t\right). \tag{15}$$

The first derivative of ϑ with respect to λ gives the average velocity $\bar{v}$ of the motor and the second derivative gives the diffusion coefficient of the motor.

From the explicit expression of this eigenvalue, the following property may be derived:

$$\vartheta(\lambda) = \vartheta(-\Psi - \lambda), \tag{16}$$

which is the Gallavotti-Cohen fluctuation theorem. Other equivalent forms of this relation can be obtained. One of them involves the large deviation function of the current v denoted $G(v)$, defined in the long time limit as

$$P(\frac{n}{t} = v) \sim e^{-G(v)t}. \tag{17}$$

The analytical expression of this function, obtained in Ref. [37], has a complicated non-linear expression in terms of the rates, but it satisfies a surprisingly simple relation:

$$G(v) - G(-v) = \Psi v. \tag{18}$$

This relation implies that the ratio of the probabilities to observe a velocity v or $-v$ after a time t satisfies the relation

$$\frac{\mathcal{P}(\frac{n}{t} = v)}{\mathcal{P}(\frac{n}{t} = -v)} = e^{-\Psi v t}. \tag{19}$$

Using Eq. (18), and the fact that $G(v)$ and $\vartheta(\lambda)$ are Legendre transforms of each other, one recovers indeed the relation (16).

The relations (16), (18) and (19) are equivalent forms of a constraint imposed on the system by the Gallavotti-Cohen fluctuation theorem. This theorem itself is a consequence of the time-reversal symmetry of the physical laws involved in this model. This symmetry is a fundamental property that does not depend on the details of the system and therefore, in this sense, the fluctuation theorem appears as a universal requirement, just as thermodynamic constraints are universal for

systems at equilibrium regardless of their microscopic structure. Of course, universality does not imply that the constraints are easy to find and to formulate explicitly for a given problem. Here, the relation (19) is an explicit prediction derived from the fluctuation theorem for molecular motors. It would be of great interest to verify this relation experimentally. Conversely, this equation can be used to measure the affinity Ψ, and therefore to access indirectly the microscopic rates, for a given molecular motor.

3.1. Modeling processivity at the single motor level

Experiments on single molecular motors depend on an important property of these motors called processivity. Molecular motors like kinesins, which can hydrolyze a large number of ATP molecules before detaching from microtubules, are called processive, whereas those like myosins II, which detach and reattach frequently from actin filaments are called non-processive. There are several ways to define processivity, either it can be defined as the average lifetime of the motor on the filament, or from the average length spanned by the motor or from the average number of ATP molecules consumed before detaching. In single molecule experiments [66, 51], the dependence of the run-length of a single kinesin on load and on the ATP concentration has been studied. On the theoretical side, the average lifetime of a molecular motor as a function of load has been studied in [67] using the flashing ratchet model. Here we focus on the run-length, for which we derive a simple expression within the discrete two-state model presented above. Using a similar theoretical approach, the average time before observing a backward step in a discrete model of a molecular motor has been studied in Ref. [34]. More generally, in a network of discrete chemical states, there are well-known methods to calculate the average lifetime of a random walker in the presence of absorbing states [65]. These methods can be used not only to calculate the lifetime of the motor on the filament, but also the dwell times associated with the motor steps as shown in Ref. [49].

The detachment of the motor from the filament can be represented by a detachment rate κ, which depends on the local site of the filament visited by the motor. Since in the discrete model presented above, the state b is the high-energy state and a a low-energy state, we assume for simplicity that detachment only occurs from site b, which corresponds to the maxima of $U_1(x)$ in Figure 3. Because of this detachment, the motor can be no longer only in states a or b, thus we need to modify the master equation in order to conserve probability at all times. This can be done by adding an extra state corresponding to the unbound motor state, which is an absorbing state. We define the generating functions $F_i(\lambda, t)$ as before, but now the matrix of evolution of these generating function is the following 3×3 matrix:

$$\mathcal{M}[\lambda] = \begin{bmatrix} -\overrightarrow{\omega_a} - \overleftarrow{\omega_a} & e^{\lambda}\overleftarrow{\omega_b} + e^{-\lambda}\overrightarrow{\omega_b} & 0 \\ e^{\lambda}\overleftarrow{\omega_a} + e^{-\lambda}\overrightarrow{\omega_a} & -\overleftarrow{\omega_b} - \overrightarrow{\omega_b} - \kappa & 0 \\ 0 & \kappa & 0 \end{bmatrix}.$$

This matrix has three eigenvalues μ_1, μ_2 and 0, which is associated with the absorbing state. The corresponding eigenvectors are $|\mu_1\rangle$, $|\mu_2\rangle$ and $|c\rangle$. If the initial state vector is $|F(\lambda,0)\rangle = A|\mu_1\rangle + B|\mu_2\rangle + C|c\rangle$, the state vector at time t is $|F(\lambda,t)\rangle = Ae^{\mu_1 t}|\mu_1\rangle + Be^{\mu_2 t}|\mu_2\rangle + C|c\rangle$. Since μ_1 and μ_2 are strictly negative, at time $t \to \infty$, $\langle e^{-\lambda n}\rangle = \langle 0|F(\lambda,\infty)\rangle = C(\lambda)$, with $\langle 0| = (1,1,1)$. Note that $C(\lambda)$ contains all the moments of the run length, and in particular the average run length, which is, in units of the lattice period,

$$\langle n\rangle = -\frac{\partial C(\lambda)}{\partial \lambda}|_{\lambda=0}. \tag{20}$$

The function $C(\lambda)$ can be calculated by projecting the left eigenvector associated with the eigenvalue 0, $\langle c|$, onto the initial state vector $|F(\lambda,0)\rangle$. If the initial state vector is along the unit vector $\mathbf{e}_x$, then one obtains

$$C(\lambda) = \frac{\overrightarrow{\omega}_a e^{\lambda} + \overleftarrow{\omega}_a e^{-\lambda}}{r\omega_a + \overrightarrow{\omega}_a \overrightarrow{\omega}_b (1-e^{2\lambda}) + \overleftarrow{\omega}_a \overleftarrow{\omega}_b (1-e^{-2\lambda})}. \tag{21}$$

If the initial state vector is along the unit vector $\mathbf{e}_x$, then

$$\langle n\rangle = \frac{\overrightarrow{\omega}_a - \overleftarrow{\omega}_a}{\omega_a + \omega_b} + 2\frac{\overrightarrow{\omega}_a \overrightarrow{\omega}_b - \overleftarrow{\omega}_a \overleftarrow{\omega}_b}{\kappa\omega_a}. \tag{22}$$

If the initial state vector is along the unit vector $\mathbf{e}_y$, then

$$\langle n\rangle = 2\frac{\overrightarrow{\omega}_a \overrightarrow{\omega}_b - \overleftarrow{\omega}_a \overleftarrow{\omega}_b}{\kappa\omega_a}. \tag{23}$$

Thus the part of the average length which is independent of the initial condition is

$$\langle \bar{n}\rangle = 2\frac{\overrightarrow{\omega}_a \overrightarrow{\omega}_b - \overleftarrow{\omega}_a \overleftarrow{\omega}_b}{\kappa\omega_a} = \frac{\bar{v}}{\kappa P_b}, \tag{24}$$

where $\bar{v}$ is the average motor velocity defined before and P_b the stationary probability to be in state b when $\kappa = 0$.

Note that it has been assumed implicitly that the motor runs in the positive direction so that by construction $\bar{v} > 0$, $\langle \bar{n}\rangle$ is positive and has the familiar form obtained above. The application of fluctuation relations to non-processive motors has not been discussed in the literature to our knowledge. We believe that a fluctuation relation will be obeyed only if a reattachment process is taken into account in the model. In this case, there is no longer an absorbing state.

3.2. Mechanochemical coupling for the discrete model

We have so far only discussed the form of fluctuation relations for models containing a single cycle. It is well known that models with at least two cycles must be introduced to account for experimental data such as those represented in Figure 5. In order to discuss more general fluctuation relations, and to compute in a simple way the chemical current, r, associated with the average ATP consumption rate, it is necessary to include in the description of the state of the motor, a chemical variable y associated with the average number of ATP consumed as done in

Eq. (9). With the notations, $\omega_a^l = \overrightarrow{\omega}_a^l + \overleftarrow{\omega}_a^l$ and $\omega_a = \overrightarrow{\omega}_a + \overleftarrow{\omega}_a$ (and similarly for site b), one obtains the chemical current

$$r = \frac{\omega_a^1 \omega_b - \omega_b^{-1} \omega_a}{\omega_a + \omega_b}, \tag{25}$$

in agreement with the cycle representation of Figure 9 and with the formula (11) above.

When the form of these rates is explicitly given in terms of the normalized force f and the normalized chemical potential $\Delta\mu$, a new reformulation of Eq. (12) is obtained:

$$k_B T \ln \frac{\overrightarrow{\omega}_b^{-l} \overrightarrow{\omega}_a^{l'}}{\overleftarrow{\omega}_a^{l} \overleftarrow{\omega}_b^{-l'}} = F_e(2d) - \Delta\tilde{\mu}\,(l - l')\,, \tag{26}$$

with $l, l' = 0, 1$. This equation can be understood as a statement of the first law of thermodynamics at the level of elementary transitions [35, 28]. Indeed, it is possible to associate the left-hand side of this equation with the heat released by the motor into the environment (treated as a reservoir at the same temperature) during transitions (l, l'). The right-hand side can then be interpreted as the difference between the mechanical work $-F_e(2d)$ and the variation of chemical energy $\Delta\tilde{\mu}\,(l - l')$ for these transitions. The variation of internal energy is zero in this case since only transitions involved in a cycle are considered. Note that similarly to this, the generalized detailed balance condition of Eq. (8) can be also interpreted as a statement of the first law at the level of elementary transitions.

Following the same steps that lead to the fluctuation relations for models with one cycle but now for a model with two cycles, one arrives at the following relation, similar to Eq. (16):

$$\vartheta(\lambda, \gamma) = \vartheta(-\tilde{\Psi} - \lambda, -\tilde{\chi} - \gamma), \tag{27}$$

with new affinities $-\tilde{\Psi}$ and $-\tilde{\chi}$ associated with the mechanical and chemical cycles. These affinities represent a part of the expression of the entropy production rate of the motor [37], which also satisfies a fluctuation relation different from that of the currents but very much related to it.

We emphasize that the relation (27) involves *both* the mechanical and the chemical activities and that, here, a symmetry relation of the type of Eq. (16) for the mechanical variable alone is not satisfied. It is therefore essential, in deriving fluctuation relations, to take into account and include all internal variables that are coupled with one another under time-reversal. Leaving aside some relevant degrees of freedom would manifest itself as an apparent violation of this symmetry and would wrongly be interpreted as a breakdown of the fluctuation theorem.

3.3. Flashing ratchet model on a continuous space

We show in this section how the ideas developed in the previous section for the discrete two-state model can now be extended to more general continuous models, such as the flashing ratchet. There are several reasons for considering continuous models as a substitute for discrete models: first of all, continuous models contain all

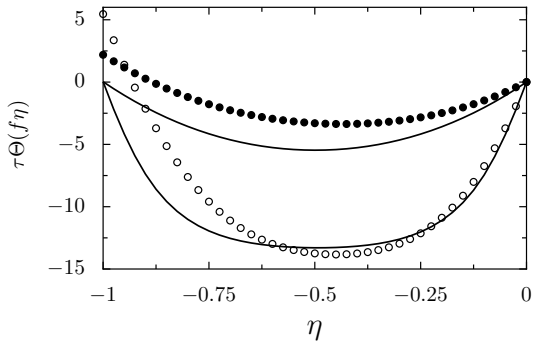

FIGURE 10. Normalized eigenvalue $\tau\Theta(f\eta)$ of the flashing ratchet model as a function of $\eta = \lambda/f$ (with $\tau = a^2/D_0$), for a normalized force $f = 5$ (top two curves) and $f = 10$ (bottom two curves). The solid curves correspond to the case where the transition rates between the internal states satisfy detailed balance, which leads to the Gallavotti-Cohen symmetry, *i.e.* to the symmetry with respect to $\eta = -1/2$. The curves with filled symbols ($f = 5$) and empty symbols ($f = 10$) correspond to the case where the detailed balance is broken with constant transition rates $\omega_1(x) = \omega_2(x) = 10\tau^{-1}$ and the same potentials.

the possible discrete models as limiting cases, second, the way to describe the effect of force on the motor is unambiguous for continuous models, and third, there are effects such as fluctuations which are not always well captured by discrete models.

We provide in this section an analytical proof that the flashing ratchet obeys a Gallavotti-Cohen symmetry [68], using a technique inspired by [17, 22]. We also analyze numerically this point by calculating the eigenvalue associated with the evolution matrix of the generating functions of the currents.

3.3.1. The purely mechanical ratchet. Before considering the case of the flashing ratchet with a mechanical and a chemical variable, it is helpful to look first at a purely mechanical ratchet, which has been used to describe in particular the translocation of a polymer through a pore [69]. In this model, one considers a random walker in a periodic potential subject to an external force F (model I) [70, 39]. The corresponding Fokker-Planck equation is

$$\frac{\partial P}{\partial t} = D_0 \frac{\partial}{\partial x}\left[\frac{\partial P}{\partial x} + \frac{U'(x) - F}{k_B T} P\right], \tag{28}$$

where $U(x)$ is a periodic potential $U(x + a) = U(x)$ and a is the period. This equation describes the stochastic dynamics of a particle in the effective potential $U_{eff}(x) = U(x) - Fx$. By solving Eq. (28) with periodic boundary conditions [69, 70], it can be readily proven that the system reaches a stationary state with

a uniform current J in the long time limit. This current is non-vanishing if a non-zero force is applied. When $F = 0$, there is no tilt in the potential, $J = 0$ and the stationary probability is given by the equilibrium Boltzmann-Gibbs factor.

Similarly to the discrete case, we introduce the generating function

$$F_\lambda(\zeta, t) = \sum_n \exp\left(\lambda(\zeta + n)\right) P((n + \zeta)a, t)\,. \tag{29}$$

The time evolution of this generating function F_λ is obtained by summing over Eq. (28). This leads to the equation

$$\frac{\partial F_\lambda(\zeta, t)}{\partial t} = \mathcal{L}(\lambda) F_\lambda(\zeta, t)\,, \tag{30}$$

where the deformed differential operator $\mathcal{L}(\lambda)$ acts on a periodic function $\Phi(\zeta, t)$ of period 1 as follows:

$$\frac{a^2}{D_0}\mathcal{L}(\lambda)\Phi = \frac{\partial^2\Phi}{\partial\zeta^2} + \frac{\partial}{\partial\zeta}\left(\tilde{U}'_{\text{eff}}\Phi\right) - 2\lambda\frac{\partial\Phi}{\partial\zeta} - \lambda\tilde{U}'_{\text{eff}}\Phi + \lambda^2\Phi\,, \tag{31}$$

where $\tilde{U}'_{\text{eff}} = a\partial_x U_{\text{eff}}/k_B T$ and the left-hand side of Eq. (31) is proportional to the inverse of the characteristic time $\tau = a^2/D_0$.

The operator $\mathcal{L}(\lambda)$ has the fundamental conjugation property

$$\mathrm{e}^{U(x)/k_B T}\mathcal{L}(\lambda)\left(\mathrm{e}^{-U(x)/k_B T}\Phi\right) = \mathcal{L}^\dagger\left(-f - \lambda\right)\Phi. \tag{32}$$

This property implies that the operators $\mathcal{L}(\lambda)$ and $\mathcal{L}^\dagger\left(-f - \lambda\right)$ are adjoint to each other, and thus have the same spectrum. If we call $\Theta(\lambda)$ the largest eigenvalue of $\mathcal{L}(\lambda)$, we obtain from Eq. (32) that $\Theta(\lambda)$ satisfies the Gallavotti-Cohen symmetry:

$$\Theta(\lambda) = \Theta(-f - \lambda). \tag{33}$$

In fact, this symmetry holds for all eigenvalues. For the special case $f = 0$, the conjugation relation (32) reduces to the *detailed balance* property [22]. One can note that this proof of the Gallavotti-Cohen symmetry does not require explicit knowledge of $\Theta(\lambda)$. In the discrete minimal ratchet model, an explicit analytical expression could be obtained for this quantity. In the continuous case, this is no longer the case but $\Theta(\lambda)$ can be calculated numerically. We have done this by first discretizing the operator $\mathcal{L}(\lambda)$ and then calculating its largest eigenvalue using the Ritz variational method [68]. A similar method has been used in Ref. [71] for the cosine potential. We note that our numerical approach can handle any form of potential.

3.3.2. The flashing ratchet. We now present the extension of the Gallavotti-Cohen symmetry to the case of the flashing ratchet model, which should include both the mechanical and chemical currents [36, 28]. When the switching rates satisfy a detailed balance condition, which is for instance the case when $\Delta\mu = 0$, the symmetry is indeed present as shown in the solid curves of Figure 10. In the general case however, where the normalized force f and chemical potential $\Delta\mu$ are both non-zero, the relation (7) is no longer satisfied and the Gallavotti-Cohen

relation (33) is not valid. This is shown in the curves with symbols in Figure 10 where for simplicity we took constant switching rates $\omega_1 = \omega_2 = 10\tau^{-1}$. For all the curves of this figure, a sawtooth potential U_1, and a potential U_2 constant in space have been chosen. The breaking of the symmetry of Eq. (33) can be interpreted as a result of the existence of internal degrees of freedom. Although other mechanisms exist which lead to violations of fluctuation relations as discussed in Ref. [74], this case appears to be rather generic.

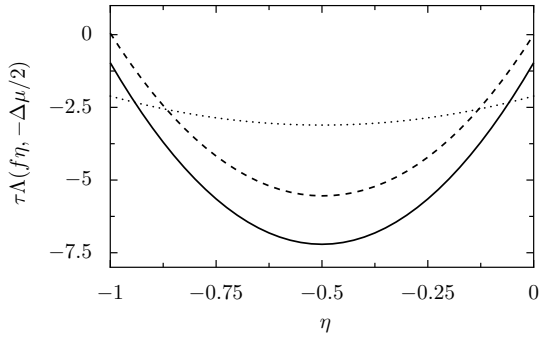

FIGURE 11. For the model described by Eqs. (34–35), the normalized eigenvalue $\tau\Lambda(f\eta, -\Delta\mu/2)$ is shown as function of η. The dashed curve corresponds to $f = 5$ and $\Delta\mu = 0$, the solid curve corresponds to $f = 5$ and $\Delta\mu = 10$, and the dotted curve corresponds to $f = 2$ and $\Delta\mu = 10$. The symmetry is recovered in all cases in this description which includes both the mechanical and chemical degrees of freedom.

Let us now introduce the probability density $P_i(x, q; t)$ associated with the probability that at time t the ratchet is in the internal state i, at position x and that q chemical units of ATP have been consumed. The evolution equations for this probability density is obtained by modifying Eqs. (3) after taking into account the dynamics of the discrete variable q. We have

$$\frac{\partial P_1(x,q,t)}{\partial t} = (\mathcal{L}_1 - \omega_1(x))\, P_1(x,q,t) + \omega_2^{-1}(x) P_2(x, q+1, t) + \omega_2^0(x) P_2(x,q,t), \tag{34}$$

$$\frac{\partial P_2(x,q,t)}{\partial t} = (\mathcal{L}_2 - \omega_2(x))\, P_2(x,q,t) + \omega_1^0(x) P_1(x,q,t) + \omega_1^1(x) P_1(x, q-1, t). \tag{35}$$

We use a notation similar to that of Ref. [37], where $\omega_i^l(x)$ denotes the transition rate at position x from the internal state i with $l(= -1, 0, 1)$ ATP molecules

consumed. This leads to

$$\omega_1^0(x) = \omega e^{(U_1 - fx)/k_B T}\,, \tag{36}$$

$$\omega_2^0(x) = \omega e^{(U_2 - fx)/k_B T}\,, \tag{37}$$

$$\omega_1^1(x) = \psi e^{(U_1 - fx)/k_B T + \Delta\mu}\,, \tag{38}$$

$$\omega_2^{-1}(x) = \psi e^{(U_2 - fx)/k_B T}\,. \tag{39}$$

We also have $\omega_1(x) = \omega_1^0(x) + \omega_1^1(x)$ and $\omega_2(x) = \omega_2^0(x) + \omega_2^{-1}(x)$. The operators $\mathcal{L}_1$ and $\mathcal{L}_2$ act on a function Φ as

$$\mathcal{L}_i = D_0 \frac{\partial^2 \Phi}{\partial x^2} + D_0 \frac{\partial}{\partial x}\left(\frac{U_i'(x) - F}{k_B T}\,\Phi\right) \qquad i = 1, 2\,. \tag{40}$$

As above, we introduce two generating functions $F_{1,\lambda,\gamma}$ and $F_{2,\lambda,\gamma}$, depending on two parameters λ and γ which are conjugate variables to the position of the ratchet and to the ATP counter q. We have for $i = 1, 2$,

$$F_{i,\lambda,\gamma}(\zeta, t) = \sum_q \mathrm{e}^{\gamma q} \sum_n \mathrm{e}^{\lambda(\zeta+n)} P_i(a(\zeta + n), q; t). \tag{41}$$

The evolution equation for these generating functions is obtained from Eq. (35) as

$$\frac{\partial}{\partial t}\begin{pmatrix} F_{1,\lambda,\gamma} \\ F_{2,\lambda,\gamma} \end{pmatrix} = \mathcal{L}(\lambda, \gamma)\begin{pmatrix} F_{1,\lambda,\gamma} \\ F_{2,\lambda,\gamma} \end{pmatrix}, \tag{42}$$

with the operator $\mathcal{L}(\lambda, \gamma)$ decomposed as

$$\mathcal{L}(\lambda, \gamma) = \mathcal{D}(\lambda) + \mathcal{N}(\gamma), \tag{43}$$

with $\mathcal{D}(\lambda)$ the diagonal matrix $\mathrm{diag}(\mathcal{L}_1(\lambda) - \omega_1, \mathcal{L}_2(\lambda) - \omega_2)$, where the deformed operators $\mathcal{L}_1(\lambda)$ and $\mathcal{L}_2(\lambda)$ have the form written in Eq. (31) with $U_{eff}(x)$ given by $U_i(x) - Fx$ for $i = 1, 2$, respectively. The operator $\mathcal{N}(\gamma)$ is defined as

$$\mathcal{N}(\gamma) = \begin{pmatrix} 0 & \omega_2^0 + \omega_2^{-1} e^{-\gamma} \\ \omega_1^0 + \omega_1^1 e^{\gamma} & 0 \end{pmatrix}. \tag{44}$$

Consider now the diagonal matrix Q defined by $\mathrm{diag}(e^{-U_1/k_B T}, e^{-U_2/k_B T})$. By direct calculation, one can verify that $Q^{-1}\mathcal{N}(\gamma)Q = \mathcal{N}^\dagger\left(-\Delta\mu - \gamma\right)$. From Eq. (32), one obtains $Q^{-1}\mathcal{D}(\gamma)Q = \mathcal{D}^\dagger\left(-\Delta\mu - \gamma\right)$. By combining these two equations, we conclude that

$$Q^{-1}\mathcal{L}(\lambda, \gamma)Q = \mathcal{L}^\dagger\left(-f - \lambda, -\Delta\mu - \gamma\right), \tag{45}$$

which leads to the Gallavotti-Cohen symmetry:

$$\Lambda(\lambda, \gamma) = \Lambda\left(-f - \lambda, -\Delta\mu - \gamma\right), \tag{46}$$

where $\Lambda(\lambda, \gamma)$ is the largest eigenvalue of $\mathcal{L}(\lambda, \gamma)$. This relation is the equivalent of Eq. (27), which was derived for the discrete model. If we consider only the mechanical displacement of the ratchet, the relevant eigenvalue $\Theta(\lambda)$ is given by $\Theta(\lambda) = \Lambda(\lambda, 0)$, which clearly does not satisfy the fluctuation relation of the form Eqs. (16–19) as shown in Figure 10. In Figure 11, we have computed $\Lambda(f\eta, -\Delta\mu/2)$ for the same potentials and with rates $\omega_i^l(x)$ of the form given above with $\omega(x) =$

$5\tau^{-1}$ and $\phi(x) = 10\tau^{-1}$. We have verified that in all cases the symmetry of Eq. (46) holds.

To conclude this section on the continuous flashing ratchet, we emphasize the following two points: (i) we have proved that the flashing ratchet satisfies the fluctuation theorem without having to adjust any parameter in the system to enforce the validity of this theorem. The only constraints on the switching rates were given *a priori* from thermodynamics and kinetic theory and these requirements are always taken into account in the very definition of the model (see, e.g., [40]). What we have shown is that these thermo-kinetic constraints are enough to imply the Gallavotti-Cohen symmetry, which itself has far-reaching consequences on the model. (ii) In order to derive the fluctuation theorem, all relevant microscopic degrees of freedom must be involved. For example, in the flashing rachet model, the position variable alone does not obey the fluctuation theorem and the chemical variable that counts how many ATP molecules have been consumed by the motor during its displacement has to be taken into account. The Gallavotti-Cohen symmetry thus leads to global mechano-chemical constraints on the modes of operation of the motor.

4. Conclusions

A first simple and useful message to take from this study is that the dynamics of a molecular motor can be described by the evolution of a random walker in an effective potential $U_{eff}(x, y)$ where x is the mechanical variable and y is the chemical variable [75]. The periodicity of the potential along x and y implies that the potential has an egg-carton shape.

The symmetry of the fluctuation relations for the currents is valid in general for the flashing ratchet model only when internal degrees of freedom are taken into account. This raises a fundamental question concerning the validity of fluctuation relations and their applicability to other types of ratchet models [72, 73, 4, 39]. More generally, other mechanisms exist which are known to produce deviations from fluctuation relations [74], and it would be valuable to know whether fluctuation relations can always be restored by enlarging the phase space and by modifying the dynamics accordingly.

On the experimental side, it would be very interesting to investigate fluctuation relations for molecular motors using single molecule experiments, in a way similar to what was achieved in colloidal beads or biopolymers experiments [57]-[62]. Using fluorescently labeled ATP molecules, recent experiments with myosin 5a and with the F_1-ATPase rotary motor, aim at simultaneous recording of the turnover of single fluorescent ATP molecules and the resulting mechanical steps of the molecular motor [76]. These exciting results indicate that a simultaneous measurement of the values of the mechanical and chemical variables of the motor is achievable in practice, and therefore from the statistics of such measurements it may be possible to obtain the distribution of probability to find the motor at a

specific position and with a specific number of molecules of ATP consumed. With enough statistics, one could thus in principle verify Eq. (27). Such an experimental verification would confirm that the Gallavotti-Cohen symmetry is a fundamental constraint that plays an essential role in the mechano-chemical coupling of molecular motors.

Finally, besides the Gallavotti-Cohen fluctuation theorem, many exact non-equilibrium relations have been discovered during the last decade, the most famous one being the Jarzynski identity [16] and its generalization by Crooks [19]. These identities, originally derived for systems being driven out of a state of thermodynamic equilibrium, have been extended by Hatano-Sasa to systems prepared in non-equilibrium stationary states and following Markovian dynamics [77]. This more general fluctuation relation leads with a proper choice of observables to generalizations of the well-known fluctuation-dissipation phenomenon known for systems close to equilibrium [78, 79, 80, 81]. These generalized fluctuation-response relations hold for systems prepared in non-equilibrium stationary states and following Markovian dynamics. The implications of the Crooks fluctuation theorem for kinesin has been analyzed in Ref. [82], while the implications of generalized fluctuation-response relations for molecular motors have been considered recently [83, 84].

All these various relations can be interpreted as universal constraints that have to be obeyed by systems far from equilibrium regardless of their detailed structure. It would be of great interest to explore the consequences of these relations in the field of ratchet models (both at the single motor level and at the level of many motors) and to draw from them some measurable predictions that could be verified experimentally on molecular motors.

Acknowledgment

D.L. acknowledges support from the Indo-French Center CEFIPRA (grant 3504-2), and the IIT Kanpur for hospitality during the 2010 Golden Jubilee.

References

[1] B. Duplantier, in *Einstein,* 1905–2005*: Poincaré Seminar* 2005, edited by T. Damour, O. Darrigol, B. Duplantier, and V. Rivasseau (Birkhäuser Verlag AG, 2006), Vol. 47 of *Prog. in Math. Physics*, pp. 201–293.

[2] R. P. Feynman, R. B. Leighton, and M. Sands, *The Feynman Lectures on Physics I* (Reading, MA, Addison-Wesley, 1963).

[3] L. Brillouin, J. Appl. Phys. **22** (1951), 334.

[4] P. Reimann, Phys. Rep. **361** (2002), 57.

[5] C. V. den Broek, P. Meurs, and R. Kawai, New J. of Phys. **7** (2005), 10.

[6] M. O. Magnasco, Phys. Rev. Lett. **71** (1993), 1477, *ibid* Phys. Rev. Lett. **72** (1994), 2656.

[7] A. Ajdari and J. Prost, C. R. Acad. Sci. Paris II **315** (1993), 1635.

[8] R. D. Astumian, Science **276** (1997), 917.

[9] K. Sekimoto, J. Phys. Soc. Jpn. **66** (1997), 1234, *ibid.* Phys. Rev. E, **76** (2007), 060103(R).

[10] J. M. R. Parrondo and B. J. D. Cisneros, Appl. Phys. A **75** (2002), 179.

[11] J. Howard, *Mechanics of Motor Proteins and the Cytoskeleton*, (Sinauer Associates, Sunderland, MA, 2001).

[12] Y. Aghababaie, G. Menon, and M. Plischke, Phys. Rev. E **59** (1999), 2578.

[13] D. Chowdhury, A. Basu, A. Garai, P. Greulich, K. Nishinari, A. Schadschneider, and T. Tripathi, Eur. Phys. J. B **64** (2008), 593.

[14] M. Müller, S. Klumpp, and R. Lipowsky, Proc. Natl. Acad. Sci. **105** (2008), 4609.

[15] G. Gallavotti and E. G. D. Cohen, Phys. Rev. Lett. **74** (1995), 2694.

[16] C. Jarzynski, Phys. Rev. Lett. **78** (1997), 2690.

[17] J. Kurchan, J. Phys. A: Math. Gen. **31** (1998), 3719, *ibid.* J. Stat. Mech. (2007) P07005.

[18] D. Evans and D. Searles, Adv. Phys. **51** (2002), 1529, *ibid.* Phys. Rev. E **50** (1994), 1645.

[19] G. E. Crooks, Phys. Rev. E **61** (2000), 2361.

[20] C. Jarzynski, Eur. Phys. J. B **64** (2008), 331.

[21] F. Ritort, Adv. Chem. Phys. **137** (2008), 31.

[22] J. L. Lebowitz and H. Spohn, J. Stat. Phys. **95** (1999), 333.

[23] B. Derrida, J. Stat. Mech. (2007), p. P07023.

[24] H. Qian, Phys. Rev. E **64** (2001), 022101.

[25] H. Qian, J. Phys.: Cond. Mat. **17** (2005), S3783.

[26] R. Chetrite and K. Gawedzki, Comm. Math. Phys. **282** (2008), 469.

[27] C. Bustamante, J. Liphardt, and F. Ritort, Phys. Today **58** (2005), 43.

[28] T. Schmiedl, T. Speck, and U. Seifert, J. Stat. Phys. **128** (2007), 77.

[29] F. Jülicher, A. Ajdari, and J. Prost, Rev. Mod. Phys. **69** (1997), 1269.

[30] A. Kolomeisky and M. Fisher, Annu. Rev. Phys. Chem. **58** (2006), 675.

[31] R. Lipowsky, Phys. Rev. Lett. **85** (2000), 4401.

[32] U. Seifert, Europhys. Lett. **70** (2005), 36.

[33] K. Sekimoto, Prog. of Theo. Phys. **130** (1998), 17.

[34] D. Andrieux and P. Gaspard, Phys. Rev. E **74** (2006), 011906.

[35] R. Lipowsky and S. Liepelt, J. Stat. Phys. **130** (2008), 39.

[36] A. W. C. Lau, D. Lacoste, and K. Mallick, Phys. Rev. Lett. **99** (2007), 158102.

[37] D. Lacoste, A.W.C. Lau, and K. Mallick, Phys. Rev. E **78** (2008), 011915.

[38] W. de Roeck and C. Maes, Phys. Rev. E **76** (2007), 051117.

[39] P. Hänggi and F. Marchesoni, Rev. Mod. Phys. **81** (2009), 387.

[40] A. Parmeggiani et al., Phys. Rev. E **60** (1999), 2127.

[41] H. Wang, C. S. Peskin, and T. C. Elston, J. Theor. Biol. **221** (2003), 491.

[42] A. Kolomeisky and B. Widom, J. Stat. Phys. **93** (1998), 633.

[43] M. Fisher and A. Kolomeisky, Proc. Natl. Acad. Sci. **96** (1999), 6597, *ibid.*, **98** (2001), 7748.

[44] Y. Kafri et al., Biophys. J.**86** (2004), 3373.

[45] C. Jarzynski and O. Mazonka, Phys. Rev. E **59** (1999), 6448.

[46] M. Schnitzer and S. Block, Nature **388** (1997), 386.

[47] T. Schmiedl and U. Seifert, Eur. Phys. Lett. **83** (2008), 30005.

[48] K. Visscher, M. J. Schnitzer, and S. M. Block, Nature **400** (1999), 189.

[49] A. Valleriani, S. Liepelt, and R. Lipowsky, Eur. Phys. Lett. **82** (2008), 28011.

[50] R. Lipowsky, S. Liepelt, and A. Valleriani, J. Stat. Phys. **135** (2009), 951.

[51] N. Carter and R. Cross, Nature **435** (2005), 308.

[52] S. Liepelt and R. Lipowsky, Phys. Rev. E **79** (2009), 011917.

[53] K. I. Skau, R. B. Hoyle, and M. S. Turner, Biophys. J. **91** (2006), 2475.

[54] P. Gaspard and E. Gerritsma, J. Theo. Biol. **247** (2007), 672.

[55] L. Mollazadeh-Beidokhti, J. Deseigne, D. Lacoste, F. Mohammad-Rafiee and H. Schiessel, Phys. Rev. E **79** (2009), 031922.

[56] E. Gerritsma and P. Gaspard, arXiv:0904.4218 (2009).

[57] J. Liphardt, S. Dumont, S. Smith, I. Tinoco, and C. Bustamante, Science **296** (2002), 1832.

[58] D. Collin, F. Ritort, C. Jarzynski, S. B. Smith, I. Tinoco, and C. Bustamante, Nature **437** (2005), 231.

[59] E. Trepagnier, C. Jarzynski, F. Ritort, G. Crooks, C. Bustamante, and J. Liphardt, Proc. Natl. Acad. Sci. USA **101** (2004), 15038.

[60] A. Imparato, L. Peliti, G. Pesce, G. Rusciano, and A. Sasso, Phys. Rev. E **76** (2007), 050101.

[61] V. Blickle, T. Speck, L. Helden, U. Seifert, and C. Bechinger, **96** (2006), 070603.

[62] J. R. Gomez-Solano, A. Petrosyan, S. Ciliberto, R. Chetrite, and K. Gawedzki, Phys. Rev. Lett. **103** (2009).

[63] J. Schnakenberg, Rev. Mod. Phys. **48** (1976), 571.

[64] D. Andrieux and P. Gaspard, J. Stat. Phys. **127** (2007), 107.

[65] T. Hill, *Free Energy Transduction and Biochemical Cycle Kinetics*, (Springer-Verlag, New York, 1989).

[66] M. J. Schnitzer, K. Visscher, and S. M. Block, Nature Cell Biol. **2** (2000), 718.

[67] A. Parmeggiani, F. Jülicher, L. Peliti, and J. Prost, Europhys. Lett. **56** (2001), 603.

[68] D. Lacoste and K. Mallick, Phys. Rev. E **80** (2009), 021923.

[69] D. K. Lubensky and D. R. Nelson, Biophys. J. **77** (1999), 1824.

[70] H. Risken, *The Fokker-Planck Equation* (Springer, Berlin, 1989).

[71] J. Mehl, T. Speck, and U. Seifert, Phys. Rev. E **78** (2008), 011123.

[72] G. Oshanin, J. Klafter and M. Urbakh, Europhys. Lett. **68** (2004), 26.

[73] F. Slanina, Europhys. Lett. **84** (2008), 50009.

[74] S. Rahav and C. Jarzynski, J. Stat. Mech-Theory E (2007), p. P09012.

[75] D. Keller and C. Bustamante, Biophys. J. **78** (2000), 541.

[76] Y. Ishii and T. Yanagida, HFSP J. **1** (2007), 15.

[77] T. Hatano and S.-I. Sasa, Phys. Rev. Lett. **86** (2001), 3463.

[78] J. Prost, J.-F. Joanny, and J. M. R. Parrondo, Phys. Rev. Lett. **103** (2009), 090601.
[79] R. Chetrite, G. Falkovich, and K. Gawedzki, J. Stat. Mech. (2008), p. P08005.
[80] T. Speck and U. Seifert, Europhys. Lett. **74** (2006), 391.
[81] M. Baiesi, C. Maes, and B. Wynants, Phys. Rev. Lett. **103** (2009), 010602.
[82] E. A. Calzetta, Eur. Phys. J. B. **68** (2009), 601.
[83] G. Verley, K. Mallick, and D. Lacoste, manuscript in preparation (2010).
[84] U. Seifert, Phys. Rev. Lett. **104** (2010) 138101.

David Lacoste
Laboratoire de Physico-Chimie Théorique
UMR 7083 CNRS
10, rue Vauquelin
F-75231 Paris Cedex 05, France
e-mail: david.lacoste@gmail.com

Kirone Mallick
Institut de Physique Théorique
CEA Saclay
F-91191 Gif sur Yvette, France
e-mail: Kirone.Mallick@cea.fr